Focusing of internal waves and the absence of eigenmodes

Leo R.M. Maas

Netherlands Institute for Sea Research, P.O. Box 59, 1790 AB Texel, The Netherlands

Abstract The spatial structure of inviscid, monochromatic, internal waves in a uniformly stratified fluid is governed by the wave equation in spatial coordinates. Following *Magaard* (1962), solutions for this equation can be constructed by means of a recursive mapping. Solutions for a closed domain with supercritical side walls suggest that internal waves get focused to a fixed limiting trajectory, irrespective of the location where energy is introduced. As the focusing is accompanied by amplitude growth, this thus offers a mechanism by which 'mixing at a distance', along certain very special ray paths, may be accomplished. The location of the attracting trajectory is a fractal function of the frequency of the monochromatic wave. Solutions exist for *any* frequency of the wave field and thus no specific spatial patterns, 'eigenmodes', prevail.

Introduction

It is a well-known feature of plane internal waves, propagating through a uniformly-stratified fluid, that they retain their angle with respect to the horizontal upon reflection from a sloping bottom (*Phillips,* 1977). For a wave entering a subcritically sloping wedge (having a slope which is less than that of the energy flux vector) the reflecting wave, bouncing back and forth between bottom and surface, propagates into the wedge, see Figure 1. Upon each reflection from the bottom the amplitude and wavenumber increase and will eventually become so large that they will give rise to nonlinear and / or viscous effects. This implies that the energy, which the incoming wave field carries, will be deposited there and will locally contribute to mixing (*Wunsch,* 1968, 1969). If the basin, however, has a supercritical side-wall, incoming internal waves will be reflected back into the deep-sea region. It seems legitimate to wonder what happens if the (2D) basin consists of two opposing supercritical side-walls. Because, in that case, neither of the two corner regions will 'attract' the incoming internal wave, one might anticipate that the internal wave will be engaged in some complex process of criss-crossing of the basin. What exactly its ray path will be, however, is not immediately obvious.

When one looks for a stationary internal wave pattern of a particular frequency in an enclosed basin its streamfunction is determined by a hyperbolic equation in spatial coordinates that vanishes at the boundary. *Cushman-Roisin et al.* (1989) and *Münnich* (1993) each developed numerical algorithms that compute the structure of these patterns. The results seem to be partly at variance with analytical results that are discussed here and, more extensively, in *Maas and Lam* (1995; ML hereafter), due to the discretization of the bottom *Magaard* (1962, 1968) showed that the partial differential equation can, remarkably, also be solved by an implicit map, which relates the new position at which a wave ray reflects from the surface to its previous position. By supplying a streamfunction-related 'field variable' (carried invariantly along the ray) in a unique interval the streamfunction field is determined completely. Magaard applied this heuristically to a subcritical domain. It turns out that the map can be obtained explicitly for some simple bottom shapes, of which only the parabola will be considered here. With some modification this map can also be used for a basin with supercritical side-walls, which enables us to address the question, raised above, quantitatively.

Bi-modal map

Consider a uniformly-stratified fluid in a parabolic basin with depth

$$H(x) = \tau(1 - x^2), \quad x \in [-1, 1] \tag{1}$$

and rigid lid at $z = 0$. The spatial structure of the streamfunction of a monochromatic wave of frequency ω is determined, in dimensionless form, by the canon-

ical hyperbolic equation (see *e.g.* ML)

$$\frac{\partial^2\psi}{\partial x^2} - \frac{\partial^2\psi}{\partial z^2} = 0, \qquad (2a)$$

where

$$\psi = 0 \quad \text{at} \quad z = 0, -H(x). \qquad (2b,c)$$

The only non-dimensional quantity still appearing in this problem, Eq. (1), is the 'virtual' depth,

$$\tau = \frac{ND}{\omega L}, \qquad (3)$$

which is the product of the aspect ratio (where D and L are the depth and half-width of the basin respectively) and the ratio of the buoyancy N and wave frequency ω. This can, alternatively, be interpreted as a scaled period of the wave. *Magaard* (1962, 1968) shows that a solution of (2a), that also vanishes at the surface, is given by

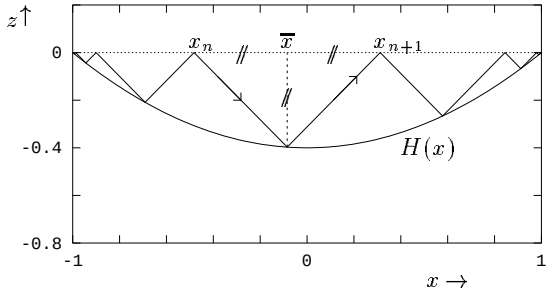

Figure 1. Sketch of a wave ray, propagating to the right in a parabolic basin given by (1) with $\tau = 0.4$.

$$\psi(x,z) = f(x-z) - f(x+z), \qquad (4)$$

for arbitrary function $f(x)$. Physically $f(x)$ is (except for a phase factor) related to the surface pressure, and its derivative to the horizontal velocity at the surface. Note that by adopting this kind of scaling the wave rays (along the directions of the characteristics $z = \pm\, x + const.$) always make an angle of 45^o with respect to the horizontal, regardless of frequency. This scaling has as its disadvantage that rays can be plotted for just one frequency at a time, but makes it easier to assess the ray diagrams. In particular, from Figure 1, it is obvious that successive surface reflections of a wave ray (denoted by x_n, $n = .., -1, 0, 1, 2, ..$) are related by

$$\frac{x_{n+1} - x_n}{2} = sH(\bar{x}), \qquad (5)$$

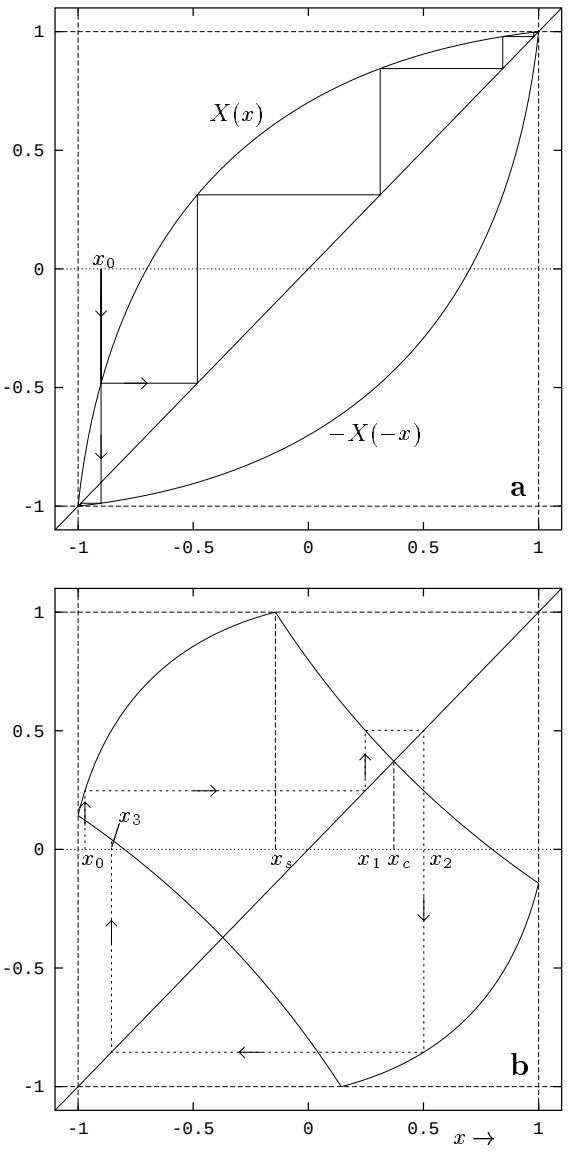

Figure 2. The bi-modal map for a) subcritical ($\tau = 0.4$) and b) supercritical ($\tau = 0.7$) values of the map parameter. Successive surface intersections are given by x_n, $n = 0, 1, 2, ...$ Special points are indicated as x_s and x_c, see Figure 3.

where $\bar{x} = (x_n + x_{n+1})/2$ and sign $s = +1, -1$ determines the two modes of the map for rightward and leftward moving characteristics respectively. The boundary condition at the bottom, $z = -H(x)$, then implies

$$f(x + H(x)) = f(x - H(x)). \qquad (6)$$

Applied at $\bar{x}$, Eq.6 and Figure 1 show that this implies that f is carried invariantly along the characteristic: $f(x_{n+1}) = f(x_n)$. From this Figure it is obvious that once we specify $f(x)$ for x-values in between two successive surface reflections of any arbitrary ray, then this function is determined over the whole interval $x \in (-1, 1)$. The parabolic bottom in (1) has maximum slope at its corners where it is $\pm 2\tau$. In the example of Figure 1 the topography is everywhere subcritical ($2\tau < 1$) and successive x_n approach the right ($s = +1$) or left ($s = -1$) corner respectively. The corners act as *attractors*. This is also evident in a graph of the map that we obtain explicitly from (5) for $H(x)$ given by (1) as

$$X(x) = -x - \frac{1}{\tau} + \sqrt{\frac{4x}{\tau} + 4 + \frac{1}{\tau^2}}. \qquad (7)$$

Here the 'rightward map' ($s = +1$) is considered and the successor of x is denoted by $X(x)$. The successor of x with a leftward map leads to $-X(-x)$.

For subcritical topographies $\tau \leq 1/2$ the rightward and leftward map are decoupled (Figure 2a), when $\tau > 1/2$, however, the corners are no longer attracting and the rightward and leftward map get coupled (Figure2b). Also, once $x > x_s$ — where x_s is the point whose rightward map brings it directly into the right-hand corner — the ray reflects downwards and its image is given by ML as

$$Y(x) = \frac{2}{\tau} - x - 2X(x). \qquad (8)$$

At the same time, once this happens, the horizontal direction in which the ray propagates should be reversed and one should shift to the leftward map (lower curves in Figures 2a,b). A similar thing happens when the ray reflects from the leftward side of the basin, and again $s \to -s$. Figure 3 gives a geometrical construction of $Y(x)$ once the direct image of x, *i.e.* X, lies outside the physical domain. Also given in this diagram are

$$x_s = \frac{2}{\tau} - 3 \qquad (9a)$$

and the point where the critical characteristic reflects from the surface

$$x_c = \frac{3}{4\tau} - \tau. \qquad (9b)$$

These two 'points' play a special role in the subsequent part of this paper.

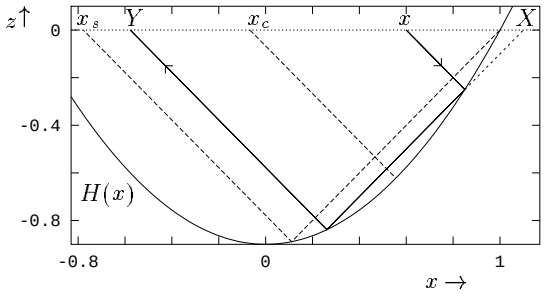

Figure 3. Construction of successive surface intersections of characteristics for a super-critically reflecting bottom. The critical characteristic (surface intersection x_c) and characteristic going through the right-hand corner (intersecting at x_s) are given by dashed lines. Note that X and Y are always eachother's images for the rightward map.

Focusing of internal waves

With the bi-modal map given, the ultimate fate of a wave-ray can be obtained by iterating it both 'forward' (initially to the right) and 'backward' (initially to the left). In this way it can be observed

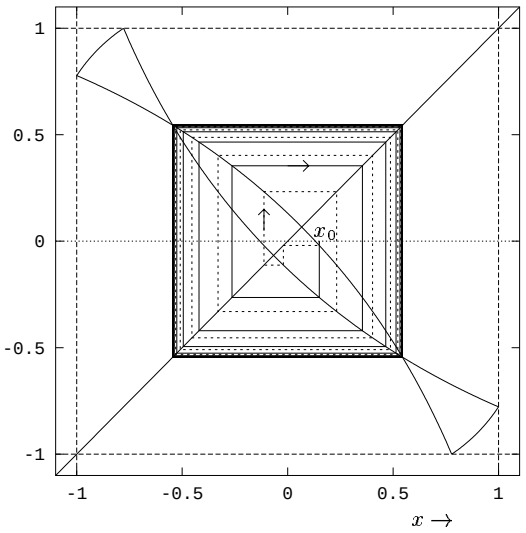

Figure 4. Bi-modal map (curved lines) and trajectories of a ray (rectangular lines) starting at x_0 for $\tau = 0.9$. Solid (dashed) lines indicate the ray that initially 'moves' to the right (left).

that the rays approach a limit cycle regardless of the

direction which they start out with. In the example of Figure 4 this is a limit cycle characterized by *two* reflections from the surface (a period-2 attractor). For even-period attractors this attractor is always unique, for odd-period attractors each attractor also has a mirror-image, but the particular attractor favored asymptotically, *i.e.* for n large, depends both on the initial location and direction which the wave ray follows (see ML; this explains why in Figure 6 below, the odd-period attractors are asymmetric: the mirrored attractor also exists, but is not reached with the initial conditions used). The approach of the attractor can, of course, also be viewed in the physical domain, which is shown, for this value of τ, in Figure 5. Independent of the direction in which the rays leave x_0 initially, the attractor is asymptotically traversed in the same sense.

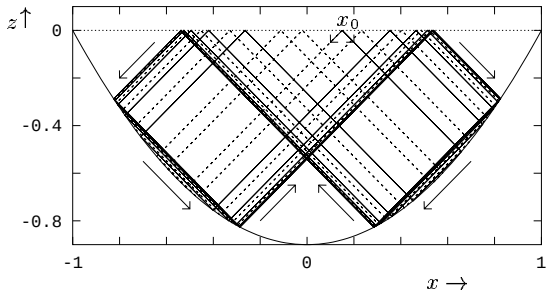

Figure 5. Construction of ray pattern for $\tau = 0.9$ and $x_0 = 0.15$ by iterated mapping. Right and leftward 'moving' characteristics are drawn as solid and dashed lines respectively. The final sense in which the limit cycle is traversed has been indicated by arrows.

The shape of the attractor is a function of the dimensionless parameter τ, the scaled period of the internal wave. A nice way of presenting this is by plotting just the surface reflections of the attractor, that is of the asymptotic state of a wave ray (n large). In Figure 6 this has been presented for values of $\tau \in (1/2, 1)$. The lower boundary of this interval is determined by the requirement that the bottom be supercritical. The upper bound is arbitrarily chosen so as to guarantee that there is always at least one ray that is reflected simply forward (this is the corner point, $x = -1$, for $\tau = 1$). A similar pattern exists, however, in the next band $\tau \in (1, 3/2)$ (ML). It is observed that there exist regions where the 'qualitative character' of the attractor (the period, say) is invariant for small variations of τ, like the period-2 attractor dis-

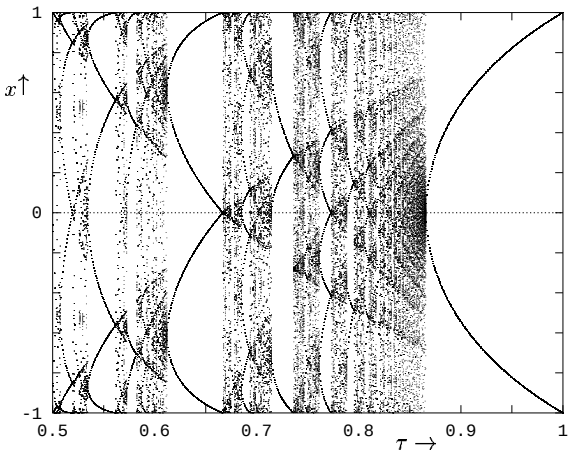

Figure 6. Plot of $x_{900} - x_{1100}$ for $x_0 = 0.123456789$ and $s = +1$ in the interval $1/2 \leq \tau \leq 1$, where τ is incremented with $1/1600$ of this interval.

cussed in Figures 4 and 5 in $1/2\sqrt{3} < \tau \leq 1$. These smooth bands are interrupted, however, by high period bands. Expansion of such bands shows that they qualitatively repeat these same features over and over again at ever reduced scales. As a function of τ the attractor, therefore, is fractal. Note that the wave rays are never diverging (chaotic), as has been verified by calculating Lyapunov exponents which are always less than or equal to zero (ML).

Specification of the wave field

It has been argued in the discussion on the subcritical parabolic bottom, Figure 1, that once $f(x)$ is specified in between any two successive reflections of an arbitrary wave ray then both $f(x)$ and, as a consequence, the streamfunction pattern are determined in the complete domain. This statement is modified in the case the bottom is (partly) supercritical and no complete classification is available yet. For the cases that the frequency (τ) is in the period-2 (or 4) band, *two* regions ('fundamental intervals') exist in which $f(x)$ can be arbitrarily specified, such that by its specification the solution is determined completely. In Figure 7 an example has been given for the period-2 region: $\tau = 0.9$. The intervals on which $f(x)$ can be freely specified are found by inspection and are given (Figure 7a) by $(-x_c, x_c)$ and $(-1, x_s)$. The latter range may also be replaced by the mirror interval $(-x_s, 1)$. It is observed that once we follow a beam of rays, originating in each of these fundamental intervals, in both the right and leftward direction

(indicated by solid and dashed lines respectively), two regions are traced out in the physical $x-z$ plane, that are complementary to each other and that each ray is ultimately approaching the attractor. This indicates

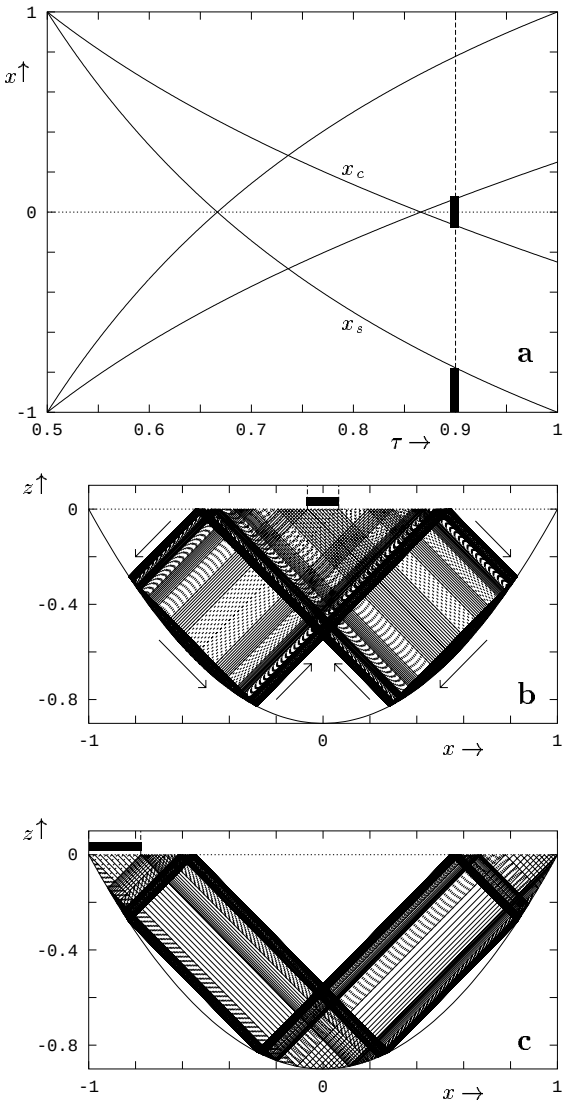

Figure 7. (a) Lines $\pm x_c(\tau)$ and $\pm x_s(\tau)$ as a function of τ. For $\tau = 0.9$ the fundamental intervals have been indicated. b) Rays coming from the inner and c) outer fundamental intervals in the specific 2-cycle case.

that once $f(x)$ is specified in the regions indicated at the top of Figures 7b and 7c, this field variable is determined over the whole region $x \in (-1, 1)$. This has been demonstrated for a particular choice of $f(x)$ in Figure 8a, being a sine, displaced differently in the

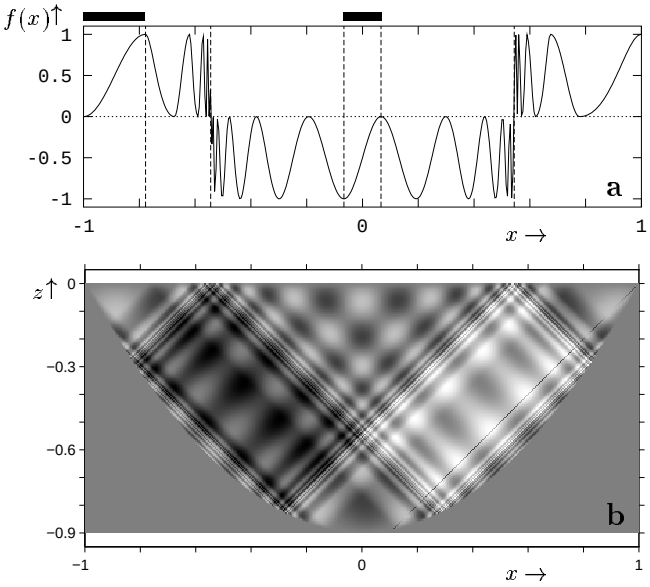

Figure 8. a) Function $f(x)$, specified in the two fundamental intervals (parts of x-axis indicated at the top, corresponding to those indicated on the dashed line of Figure 7a), and subsequently calculated values of $f(x)$ in remaining parts of domain for $\tau = 0.9$. b) Spatial structure of streamfunction field, $\psi(x, z)$, obtained from $f(x)$ with Eq. (10).

two fundamental intervals. With this function $f(x)$ the streamfunction pattern $\psi(x, z)$ of the oscillatory streamfunction $Re[\psi(x, z)e^{i\omega t}]$, where t is time, can be determined as

$$\psi = \begin{cases} f(x-z) - f(x+z) & \text{in I} \\ f(a(z-x) - x + z) - f(x+z) & \text{in II} \\ f(x-z) - f(-a(x+z) - x - z) & \text{in III,} \end{cases} \qquad (10a)$$

where regions I, II and III are defined as

$$\text{I} : \{x, z \ ; \ |x| - 1 \leq z \leq 0\}$$

$$\text{II} : \{x, z \ ; \ -H(x) \leq z < x - 1\} \qquad (10b)$$

$$\text{III} : \{x, z \ ; \ -H(x) \leq z < -x - 1\},$$

and

$$a(y) \equiv \frac{1 + \sqrt{1 + 4\tau(\tau + y)}}{\tau}. \qquad (10c)$$

For $f(x)$ real, the resulting pattern is, formally, a spatially standing internal wave pattern. As in the study of internal waves approaching a wedge (*Wunsch,* 1968, 1969) it is unlikely, however, that the waves approaching the attractor ever get back (in order to form a standing wave) as other physical processes (like

nonlinear and viscous effects), neglected sofar, will become active and drain the incoming energy flux, implying mixing along the attractor within the basin. A more correct solution would equally have to show an internal wave pattern just propagating *towards* the attractor. The technical implementation of this and the evaluation of a proper initial value problem are currently being studied.

Absence of eigenmodes

It has been expected that internal waves in enclosed stratified basins will be characterized by the existence of eigenmodes. This is suggested by the presence of such modes for the corresponding surface gravity wave problem and similar modes for interfacial waves in a two-layer fluid, referred to as internal seiches (*Defant*, 1941). Consider, for instance, the long wave modes that appear at the surface of a homogeneous fluid in a one-dimensional basin $x \in (0,1)$ of constant depth. The horizontal velocity field is determined by the wave equation

$$\frac{\partial^2 u}{\partial t^2} - \frac{c^2}{L^2}\frac{\partial^2 u}{\partial x^2} = 0. \qquad (11)$$

Here L denotes the basin length and c is the long wave speed. For monochromatic waves, $u(x) \propto e^{i\omega t}$, solutions, $u_n(x) = \sin n\pi x$, vanishing at the sides of the basin, determine a discrete set of frequencies

$$\omega'_n = n\pi,$$

where frequency has been nondimensionalized with L/c: $\omega' = \omega L/c$. The existence of eigenmodes is useful because, when they form a complete set, the forcing — which in the above example should appear at the right-hand of (11) with a spatial part $F(x)$, say — can be projected on the eigenmodes and the solution of the forced problem can subsequently be written down as the sum over the eigenmodes

$$u = \sum_{n=1}^{\infty} \frac{F_n}{\omega'^2 - \omega'^2_n} \sin n\pi x,$$

weighted with amplitudes, F_n, that are determined by the projections of the forcing

$$F_n = \int_0^1 F(x) \sin n\pi x dx.$$

Münnich (1993, 1994) noted that this correspondence breaks down once the fluid is continuously stratified. This phenomenon is foreshadowed by the degeneracy of the 'eigenmodes' that appear in a rectangular, stratified basin. For a streamfuncion field describing linear internal gravity waves, $\psi(x,z)e^{i\omega t}$, the spatial pattern is determined by

$$\frac{\partial^2 \psi}{\partial x^2} - \omega'^2 \frac{\partial^2 \psi}{\partial z^2} = 0,$$

where the wave frequency has here been normalized with the buoyancy frequency and the aspect ratio, and the rectangle is given by $x, z \in [0,1]\times[0,1]$. With vanishing streamfunction at the boundary solutions are obtained as

$$\psi(x,z) = \sin n\pi x \sin m\pi z, \qquad (12a)$$

provided

$$\omega'_{n,m} = \pm\frac{n}{m}, \qquad (12b)$$

for natural numbers n, m. As *Münnich* (1993, 1994) remarks, it is clear from (12) that, first of all, the 'eigenfrequencies' $\omega'_{n,m}$, being rational, are no longer well-seperated — they are *dense* within the real numbers — and, second, that the 'eigenmodes' are no longer unique, as any common multiple, $j \in \mathbb{N}$, of n and m leads, by (12b), to the same eigenfrequency but has a mode structure (12a) that is the j-tuple of the original mode. As is observed in ML this implies that for this geometry, in the case of forcing, we can circumvent the forward and backward discrete Fourier transform and are able to construct the solution directly from the specified forcing by means of the ray method.

These results apply also to nonrectangular basins, except that the degeneracy, as Figure 6 shows, is even worse, because 'eigenmodes' exist for frequencies within *compact* domains and are, within the fundamental intervals, completely arbitrary. Instead, for the parabola discussed here, there is just a discrete set of wave frequencies for which *no* stationary internal wave pattern exists. It is clear that by this time the 'eigenmode' has lost all its specificness and this terminology is no longer useful. The 'failure of the eigen value approach' has previously been noted by *Cushman-Roisin et al.* (1989), but the way the bottom is discretized in their numerical approach (by a set of horizontal and vertical line segments) precludes the identification of the focusing phenomenon.

Acknowledgements

The author is grateful to Peter Müller for organizing a stimulating conference. TeXnical assistence

by Frans-Peter Lam during the preparation of the manuscript is equally appreciated.

References

Cushman-Roisin, B., V. Tverberg and E.G. Pavia, 1989: Resonance of internal waves in fjords: a finite-difference model. *J. Mar. Res. 47*, 547-567.

Defant, A., 1941: *Physical Oceanography, Vol. II*, Pergamon Press.

Maas, L.R.M. and F.-P.A. Lam, 1995: Geometric focusing of internal waves, *submitted to J. Fluid Mech.*

Magaard, L., 1962: Zur Berechnung interner Wellen in Meeresräumen mit nicht-ebenen Böden bei einer speziellen Dichteverteilung. *Kieler Meeresforschungen 18*, 161-183.

Magaard, L., 1968: Ein Beitrag zur Theorie der internen Wellen als Störungen geostrophischer Strömungen. *Deutsche Hydrogr. Zeitschr. 21*, 241-278.

Münnich, M., 1993: On the influence of bottom topography on the vertical structure of internal seiches. Dissertation ETH Zürich, 97 pp.

Münnich, M., 1994: The influence of bottom topography on internal seiches in continuously stratified media. In:*Hopfinger, E. B. Voisin and G. Chavand; Preprints of the Fourth International Symposium on Stratified Flows, Vol. 2*, 8pp.

Phillips, O.M., 1977: *The dynamics of the upper ocean, 2nd ed.*, Cambridge University Press.

Wunsch, C., 1968: On the propagation of internal waves up a slope. *Deep-Sea Res. 15*, 251-258.

Wunsch, C., 1969: Progressive internal waves on slopes. *J. Fluid Mech. 35*, 131-144.